P1.23 COMPARISON OF TWO WINDSTORM EVENTS DURING THE SIERRA ROTORS PROJECT AND TERRAIN-INDUCED ROTOR EXPERIMENT

Brian J. Billings*
National Research Council, Monterey, CA

James D. Doyle
Naval Research Laboratory, Monterey, CA

1. INTRODUCTION

The main objective of the recent Terrain-induced Rotor Experiment (T-REX, Grubišić et al. 2008) was to perform a comprehensive study of the coupled mountain-wave/rotor/boundary-layer system. In addition to this scientific objective, the data sets and findings of T-REX are expected to result in improvements in mesoscale and microscale modeling and the prediction of aviation hazards, aerosol transport and dispersion, and downslope windstorms. The opportunity to observe the later phenomenon was present during a number of events during this program and its earlier pilot study: the Sierra Rotors Project (SRP, Grubišić and Billings 2007). Since the ultimate goal is an improvement in forecasting, we will utilize the National Weather Service criteria for a high wind warning. In the region of interest, this is sustained winds $\geq$ 40 mph (18 m s^{-1}) for at least 2 hours or any gust $\geq$ 58 mph (26 m s^{-1}) below 5,000' ASL.

During the four months of field observations, there were a total of eight events in which wind gusts of this magnitude were recorded. In six of these eight events, the highest wind gusts were from a westerly (downslope) direction. In this study, we examine two of these windstorm events. SRP Intensive Observing Period (IOP) 16 contained the highest wind gust observed in either of the two projects. This case was previously used as an illustration of the wave and rotor structure during SRP events in a summary by Grubišić and Billings (2008). The other case, which occurred during T-REX on 5 April 2006, was not a declared IOP, but still produced high wind gusts and was documented by some fortuitous measurements. In addition to the observations collected during the events, we will also use high-resolution numerical simulations to isolate the physical mechanisms responsible.

2. OBSERVATIONS AND SIMULATIONS

2.1 *Field Measurements*

The Sierra Rotors Project was held in March and April 2004 in Owens Valley, CA, which is located to the lee of the highest portion of the Sierra Nevada. The core instrumentation deployed during SRP can be divided into three areas. First is a permanent mesonetwork of automated surface observing stations operated by the Desert Research Institute (DRI). The DRI network consists of 16 stations which are arranged in three parallel lines running across the width of the valley floor. The average cross-valley spacing is 3.2 km. Each station reports temperature, pressure, humidity, and wind speed and direction every 30 s. The observations from this network were used to identify the high wind events enumerated in the introduction. Secondly, two NCAR Integrated Sounding Systems (ISS) were deployed to the valley to provide wind profiler observations and radiosonde launch capabilities. Finally, radiosondes were launched upstream of the valley by the Naval Air Station at Lemoore and NCAR's Mobile GPS Advanced Upper-air Sounding (MGAUS) unit. Additionally, during the majority of the project, a time-lapse video camera installed by Yale University observed cloud formations over the study area.

Owens Valley was also the site of the Terrain-induced Rotor Experiment during March and April 2006. A major improvement in the observational capabilities of this experiment was the operation of three different research aircraft. However, due to the fact that the 5 April event was not a declared IOP, there were no aircraft operations at this time, so we will focus on the ground instrumentation. The locations of all of the T-REX observation platforms used in this study is shown in Fig. 1. In addition to all of the returning instrumentation from SRP (including a third ISS unit), there were three lidars deployed to the valley: one aerosol lidar (REAL) operated by NCAR and two Doppler lidars operated by Arizona State University (ASU) and the Deutsches Zentrum für Luft- und Raumfahrt (DLR). Also, there were a number of new surface wind observations available from surface stations deployed by the University of Leeds and flux towers operated by the University of Leeds, ASU, and NCAR's Integrated Surface Flux Facility (ISFF) group. While radiosondes were not launched from Lemoore or NCAR facilities during non-IOPs, the University of Leeds did launch sondes every day at 1400 and 2300 UTC from the Independence airport and the Air Force Research Laboratory (AFRL) launched them upstream of Owens Valley at various times, including during the 5 April event. Additional instruments which were not used in the analysis of this windstorm event will not be discussed here.

2.2 *Model Setup*

During both projects, real-time numerical simulations were performed using the Naval Research Laboratory's Coupled Ocean-Atmosphere Mesoscale Predic-

* *Corresponding author address:* Brian Billings, Naval Research Laboratory, 7 Grace Hopper Ave, Monterey, CA; e-mail: brian.billings@nrlmry.navy.mil

Report Documentation Page

Form Approved
OMB No. 0704-0188

1. REPORT DATE	2. REPORT TYPE	3. DATES COVERED
JUN 2010		**00-00-2010 to 00-00-2010**

4. TITLE AND SUBTITLE	5a. CONTRACT NUMBER
Comparison of Two Windstorm Events During the Sierra Rotors Project and Terrain-Induced Rotor Experiment	5b. GRANT NUMBER
	5c. PROGRAM ELEMENT NUMBER
6. AUTHOR(S)	5d. PROJECT NUMBER
	5e. TASK NUMBER
	5f. WORK UNIT NUMBER
7. PERFORMING ORGANIZATION NAME(S) AND ADDRESS(ES) **Naval Research Laboratory,Monterey,CA,93943**	8. PERFORMING ORGANIZATION REPORT NUMBER
9. SPONSORING/MONITORING AGENCY NAME(S) AND ADDRESS(ES)	10. SPONSOR/MONITOR'S ACRONYM(S)
	11. SPONSOR/MONITOR'S REPORT NUMBER(S)

12. DISTRIBUTION/AVAILABILITY STATEMENT
Approved for public release; distribution unlimited

13. SUPPLEMENTARY NOTES
American Meteorological Society (AMS) 13th Conference on Cloud Physics, 13th Conference on Atmospheric Radiation, 28 June ? 2 July 2010, Portland, Oregon

14. ABSTRACT

15. SUBJECT TERMS

16. SECURITY CLASSIFICATION OF:			17. LIMITATION OF ABSTRACT	18. NUMBER OF PAGES	19a. NAME OF RESPONSIBLE PERSON
a. REPORT **unclassified**	b. ABSTRACT **unclassified**	c. THIS PAGE **unclassified**	**Same as Report (SAR)**	**8**	

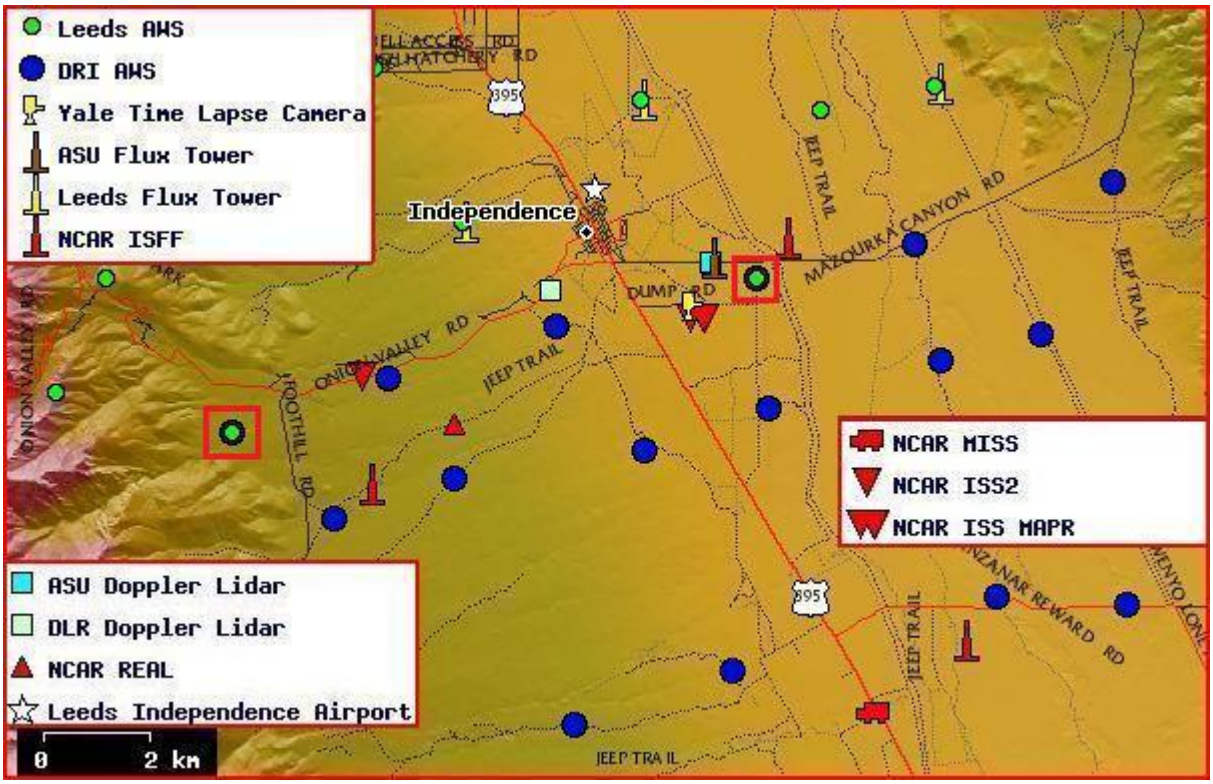

FIG. 1: Selected field instrumentation during the Terrain-induced Rotor Experiment. DRI network stations 1 and 4 are highlighted by red boxes. The MGAUS and AFRL radiosonde sites are located to the west in the Central Valley. Note that during the Sierra Rotors Project, MAPR was at the location of MISS in this figure and MISS was at the Leeds radiosonde launch site. (http://mapserver.eol.ucar.edu/trex)

tion System (COAMPS®, Hodur 1997). COAMPS is a fully compressible, non-hydrostatic model which solves the governing equations using a centered-in-time finite-difference scheme on an Arakawa-C grid and a sigma-altitude vertical coordinate system. The model uses a full set of physical parameterizations to include the effects of subgrid-scale turbulence and boundary layers, radiative heating and cooling, cumulus convection, and cloud microphysics. The lateral boundary conditions are provided by the Navy's Global Atmospheric Prediction System (NOGAPS), which also provides the first-guess field for the initial conditions, although these can be replaced by a previous COAMPS forecast for subsequent runs. For the real-time runs, data assimilation was performed using a multi-variate optimum interpolation scheme. However, more recently the NRL Atmospheric Variational Data Assimilation System (NAVDAS) has been integrated into COAMPS and is applied in these more recent runs. Simulations for the Sierra Rotors Project used two nested domains with horizontal resolutions of 9- and 3-km, while the simulations for T-REX increased to 6- and 2-km. Both real-time runs were able to forecast the occurrence of a significant westerly wind event as well as the general vertical structure of each event. However, the horizontal resolution of these simulations is most likely too coarse to resolve some of the small-scale structures involved in determining the onset and distribution of the winds in this event. Therefore, new COAMPS simulations were performed using an additional nested domain and horizontal resolutions of 9-, 3-, and 1-km.

3. CASE DESCRIPTIONS

3.1 *Sierra Rotors IOP 16*

Holmboe and Klieforth (1957) found that strong lee wave events over the southern Sierra Nevada are associated with: i) an upper trough along the Pacific Coast with strong westerly flow across the Sierra and ii) a cold front or an occluded front approaching California from the northwest. While many events fitting this pattern were observed during SRP and T-REX, SRP IOP 16 occurred in a different synoptic setting. In this case, a large-amplitude ridge was located off of the coast, while an east-west oriented shortwave trough propagated southward through the intermountain west (Fig. 2), with westerly flow ahead of trough and northerly flow behind it. This trough was associated with a strong cold front, which approached the valley from the northeast and was blocked along the east-

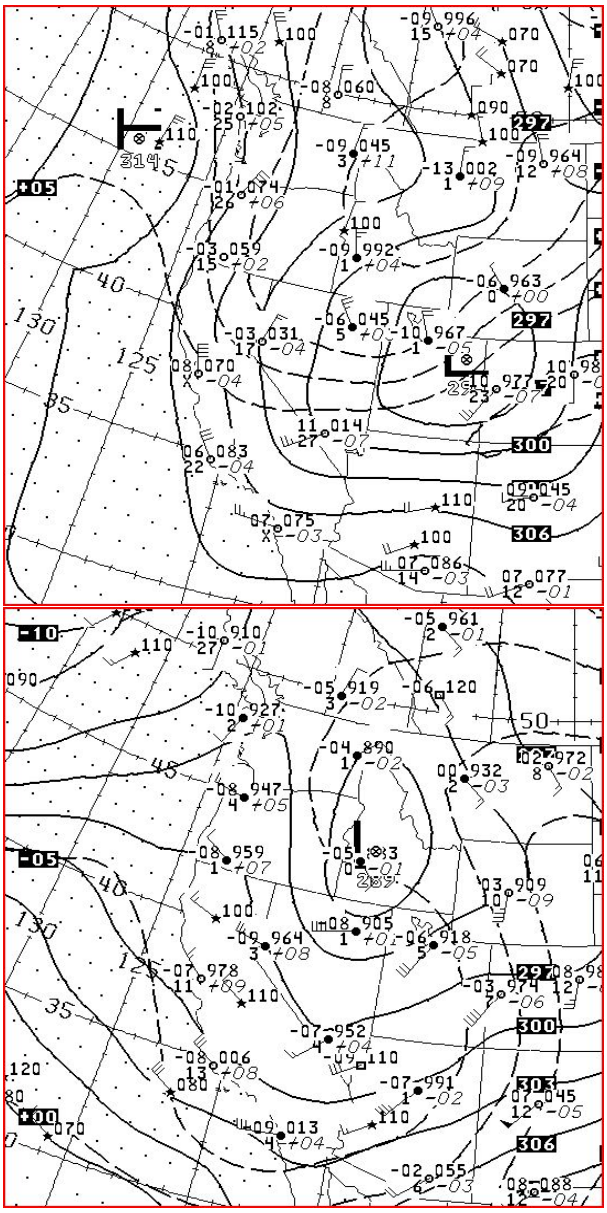

FIG. 2: 700 mb analysis for (top) 00 UTC 29 Apr 2004 and (bottom) 00 UTC 6 Apr 2006 (http://nomads.ncdc.noaa.gov).

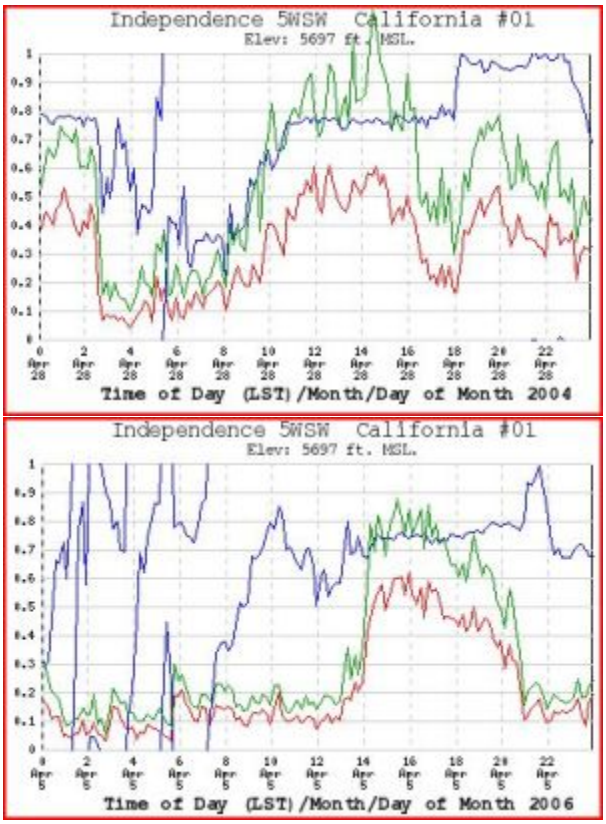

FIG. 3: Time series of average wind speed (red), maximum wind gust (green), and average wind direction (blue) from DRI network station 1 for (top) 28 April 2004 and (bottom) 5 April 2006. The y-axis gives fractions of 70 mph for speeds and 360 degrees for direction. (http://www.wrcc.dri.edu/trex)

ern side of the Sierra at the surface (not shown). While the specific synoptic pattern was atypical in this case, the basic ingredients of strong westerly flow and a pre-frontal environment were still present.

Near the bottom of the steepest slopes at DRI network station 1, strong westerly winds (gusting to 50 mph) began during the mid-afternoon of 27 April and continued until the early morning hours of the 28th before abruptly decreasing (Fig. 3). Easterly, upslope flow was observed until 08 LST (16 UTC) when gradually the direction began to shift and the speeds began to increase. From approximately 11-18 LST (19-02 UTC), the winds were westerly and quite strong with maximum average wind speeds of 42 mph and a maximum gust of 80.6 mph between 14-15 LST (22-23 UTC). Further into the valley, the onset was later and the wind speeds were lower, though still significant and often at warning criteria. Vertical profiles of the wind speed (not shown) show that the strong flow was confined to a shallow layer in the lowest 1-2 km above the surface with weaker winds above the level. The westerly flow was less obvious along the southern line of stations. The two stations at the southeast corner of the network had a significant northerly component, while the two stations at the southwest corner often observed a southerly flow (Fig. 4). This may suggest a horizontal vortex associated with a gap jet being observed by the two northern line of stations. At 18 LST (02 UTC), the direction abruptly shifted to northerly and persisted at a lower speed at station 1, but at an increased speed for many stations on the valley floor. In fact, some of the 58+ mph gusts observed during this event came from a northerly direction.

Upstream soundings from MGAUS at the time of the westerly onset (not shown) reveal a relatively unstable profile with no significant inversions in the lower to middle

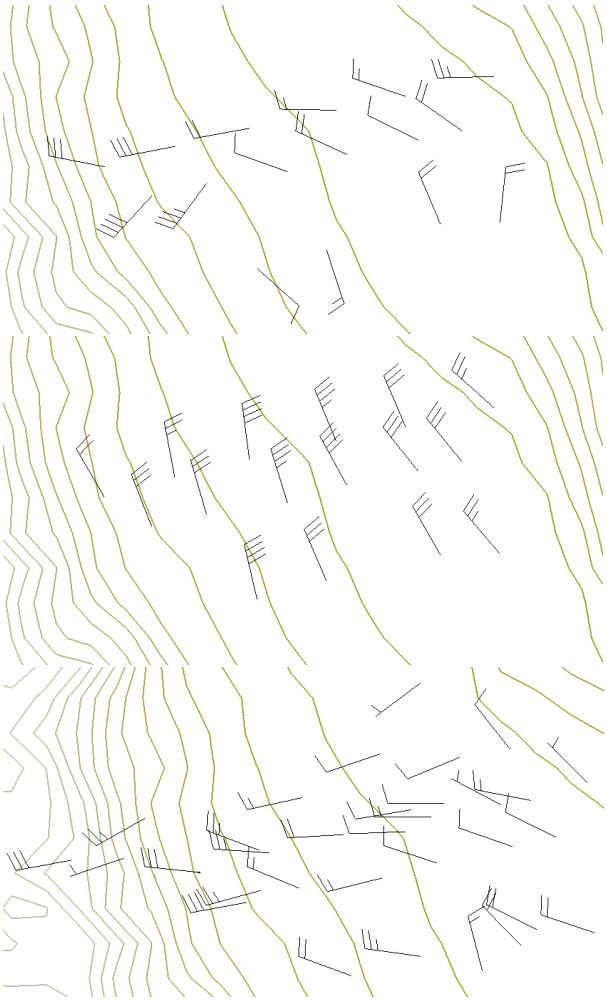

FIG. 4: Surface winds at (top) 22 UTC 28 Apr 2004, (middle) 03 UTC 29 Apr 2004, and (bottom) 00 UTC 6 Apr 2006.

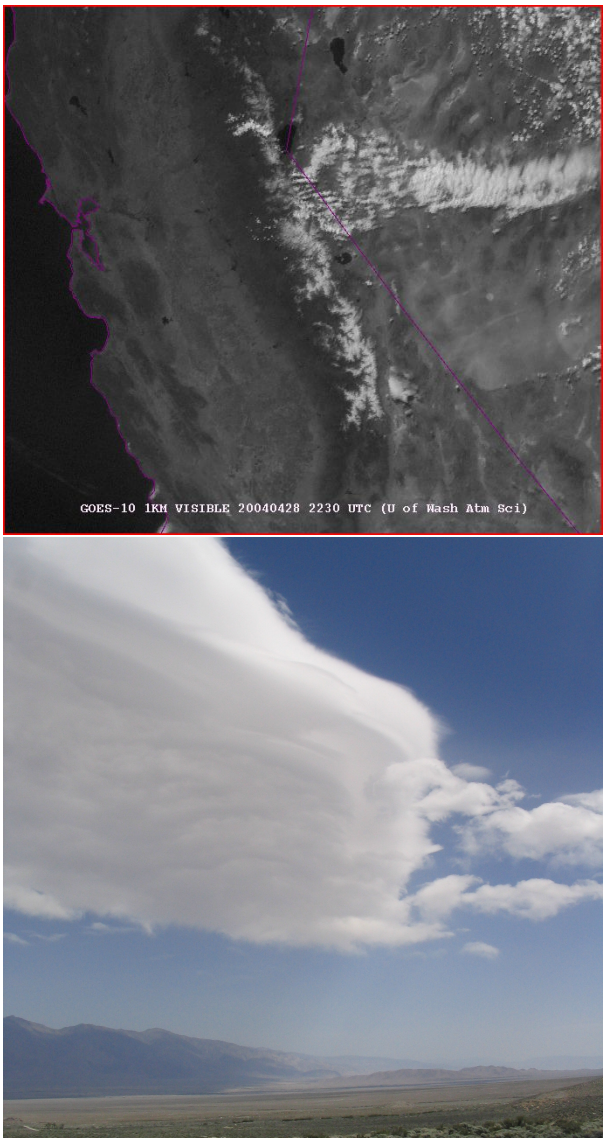

FIG. 5: (Top) visible satellite image at 2230 UTC. (Bottom) Lenticular cloud over Owens Valley at 2100 UTC looking SE (photo by Alex Reinecke).

troposphere. However, there is evidence to indicate that mountain wave and rotor activity was present over the valley. Figure 5 shows a satellite image and photograph of Owens Valley during the event. There is an isolated cloud with a leading edge over the center of the valley, consistent with a lenticular cloud associated with a long-wavelength mountain lee wave. The photograph shows that the cloud has a relatively smooth upper surface, which further supports this identification, although there are small cumulus fragments to the rear which may be caused by rotor activity. Additionally, wind profiler measurements from NCAR's Mobile ISS unit (MISS) show strong upward vertical velocities exceeding 2 m s^{-1} (Fig. 6) at the appropriate location relative to the cloud formation.

Comparing the COAMPS simulated surface wind field (not shown) with the network observations show that the model performed very well in capturing this event. The timing in the model is 1-2 hours behind the observations and there is no separation of the surface westerlies in the early morning hours, but the model does capture the period of uncoupled, thermally-driven circulations and the strong westerly winds which sweep across the entire network. Examining vertical cross-sections of the COAMPS simulation can provide insight into the onset of this westerly flow and the structure during its most intense period. Just prior to the onset (not shown), there is a large amplitude mountain wave to the immediate lee of the mountain which decays rapidly downstream. The zonal wind speed at the surface is consistent with a wave-induced pressure perturbation with weak or stagnant flow under the crests and slightly enhanced winds under the troughs. Thirty minutes later (Fig. 7a), zonal surface flow

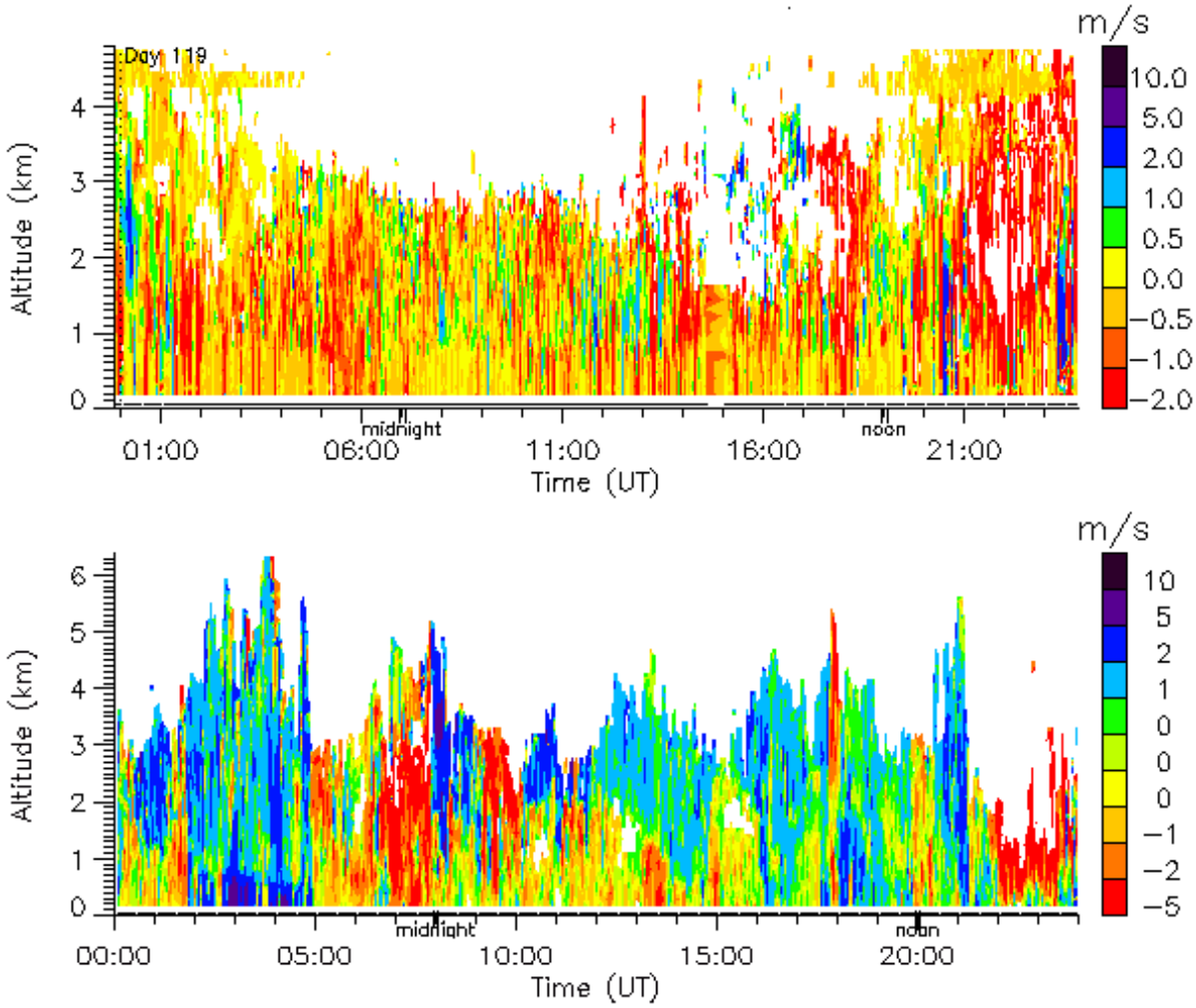

FIG. 6: Time-height series of vertical velocity from (top) MISS for 28 April 2004 and (bottom) ISS2 for 5 April 2006. Note the different color scales on these two figures.

in excess of 7.5 m s^{-1} has extended into the center of the valley and the mountain wave appears to have been reduced in amplitude. This is consistent with the effects of surface heating on boundary layer separation studied by Jiang et al. (2007), i.e. the deeper mixed layer tends to result in flow remaining attached to the surface.

After the moderately strong westerlies have entered the valley, the wave structure at upper-levels quickly breaks down and a shooting type flow develops, with much stronger westerlies entering into the valley in a shallow layer near the surface and a turbulent area of weak or reversed flow developing in the middle of the valley atmosphere (Fig. 7b). Over time, the strength of this feature intensifies and the updraft at the leading edge of the strongest surface flow extends from below 3 km to over 8 km MSL. The structure of this event is reminiscent of a case observed during the Sierra Wave Project on 25 April 1955 in which one of the project's sailplanes was destroyed after entering an extremely turbulent rotor zone (Holmboe and Klieforth 1957). There are also similarities with the analytical downslope windstorm model developed by Smith (1985) where a strong, shallow surface flow is overlain by a stagnant, turbulent region in mid-levels. After 00 UTC, the westerly flow begins to retreat westward, while simultaneously increasing in strength (not shown). The zonal wind flow exceeds 40 m s^{-1} and the turbulent kinetic energy exceeds 65 m^2 s^{-2} in the updraft. When the cold front passes over the network, there is a very abrupt shift to strong northerly flow and wave activity over the valley nearly ceases, as seen in the observations.

3.2 *T-REX 5 April Event*

Similar to SRP IOP 16, the high wind event on 5 April 2006 during T-REX did not occur while an upper-level low was located off of the Pacific coast, but instead developed while the 700 mb low center was positioned over southern Idaho (Fig. 2). The associated cold front

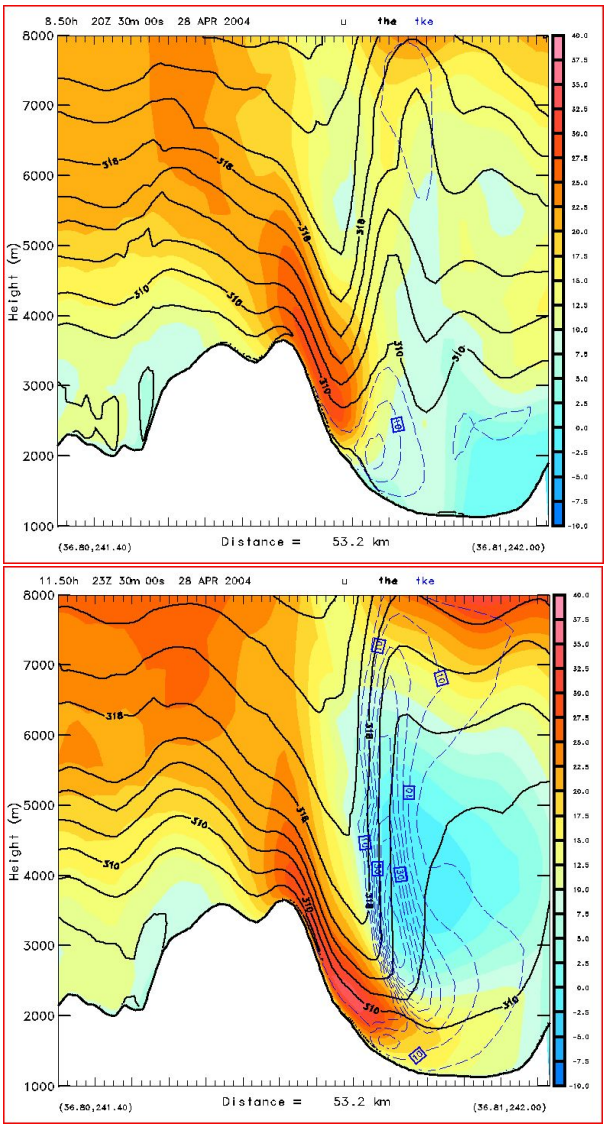

FIG. 7: Valley-normal vertical cross-section through the Independence airport of u-wind component (shaded), isentropes (solid black), and turbulent kinetic energy (dashed blue) at (top) 2030 UTC 28 April and (bottom) 2330 UTC 28 April 2004.

had already passed far to the east of Owens Valley, but a secondary trough was moving over the area during the late afternoon hours of the 5th. This trough was sharply curved at the 700-mb level so that only a brief period of westerly airflow was present across the Sierra. Prior to this, strong southerly flow with accompanying cloud and precipitation was present, while north-northwesterly flow developed at the conclusion of the event. The fact that this westerly event occurred post-frontally makes it unique to the windstorms documented during the two field campaigns.

The previous two days had been characterized by strong southerly flow and significant precipitation over the region. (Mammoth Mountain Ski Resort reported 60 inches of snow during this period.) Strong southerlies persisted over the majority of the valley through the morning of 5 April with the exception of a few stations near the base of the Sierra Nevada, such as DRI station 1 which reported light to moderate westerlies (Fig. 4). At 14 LST (22 UTC), the wind speed abruptly increased at station 1 and strong westerlies rapidly spread across the entire width of the valley. Initially, the strongest mid-valley flow was seen along the northern station lines, but later, southern stations began to observe the highest sustained wind speeds (Fig. 5). Strong westerly winds were observed at station 1 for approximately seven hours with a peak wind gust of 61.6 mph shortly before 16 LST (00 UTC 6 April). Multiple stations near the northwest and southeast corners of the network also reported a strong gust of lesser magnitude, even though they did not experience westerlies as prolonged as seen at station 1. Vertical profiles of the wind speed (not shown) show that the strong flow is confined to a shallow layer in the same manner as in SRP IOP 16.

The AFRL and University of Leeds soundings at 2300 UTC (not shown) both show little stability in the lower atmosphere beneath a strong inversion at 8 km ASL. This is consistent with satellite imagery (Fig. 8a), which contains anvils from cumulonimbus clouds scattered across the southwestern US. On the other hand, satellite also shows clouds organized in bands parallel to the mountains and lenticular clouds were present over Owens Valley, such as on the right edge of the photograph shown in Fig. 8b. Cloud spilling into the valley seem to have elements of both a convective and a downslope windstorm nature (Fig. 8c). Remote sensors also sampled the flow field during this breakthrough. NCAR's second ISS unit (ISS2) measured strong upward motion near to the surface (Fig. 6), although no returns were obtained from higher levels. This is similar to another major wind event which occurred 1-2 weeks earlier. NCAR's REAL lidar operated for a few hours during the 5 April event and a single frame from an RHI animation is shown in Fig. 9. Flow can be seen spilling down the lee slopes as well as separating from the crests, along with turbulent motion over the center of the valley. The DLR Doppler lidar also measured this strong downslope flow at various times during the afternoon hours (not shown).

As with SRP IOP 16, the COAMPS simulation for this event matches the observations well with the exception of a late timing bias and strong westerlies at 12 UTC along the lower Sierra slopes, which were not observed. This later feature was a persistent bias in the model throughout the field experiment. During the morning hours, COAMPS produces the remains of the strong southerly flow associated with the previous day's storm, while the earliest signs of westerly wind are associated with a gap jet that develops between 22-23 UTC 5 April. Vertical cross-sections through this area (Fig. 10t) show that the stronger zonal flow enters the valley in a shallow layer near the surface undercutting the valley air. This structure is similar to that documented by Jiang and

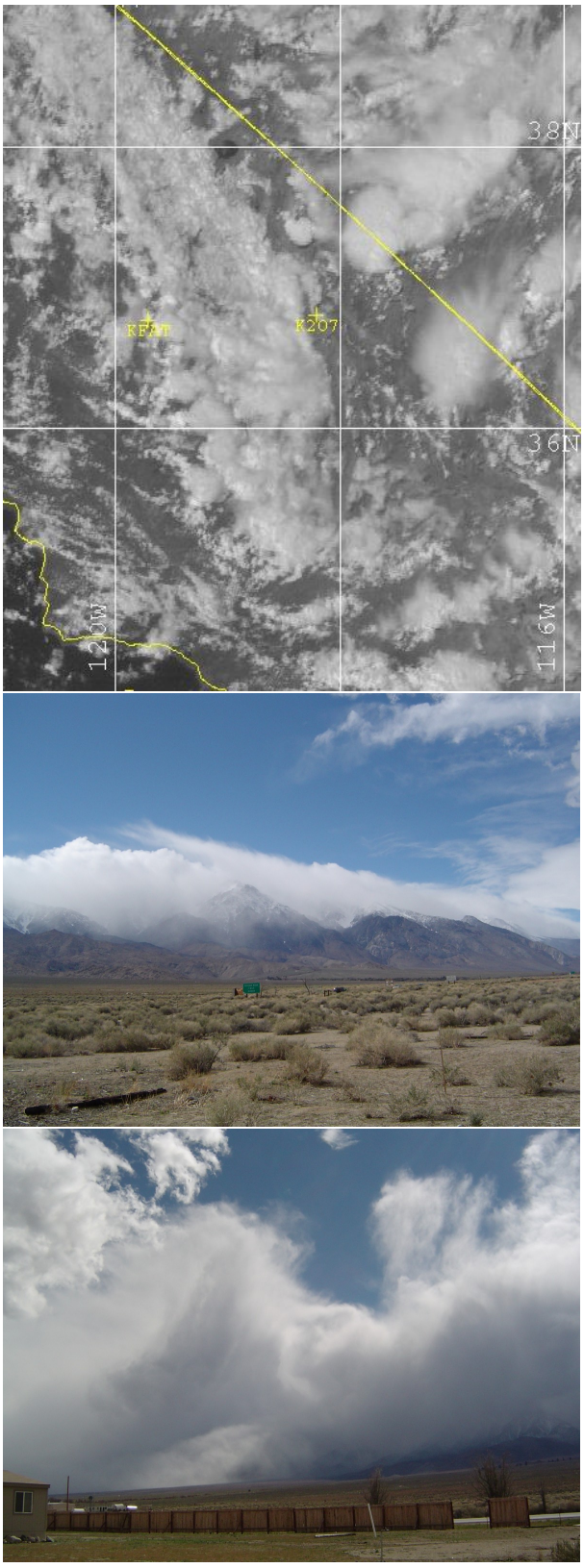

FIG. 8: (Top) visible satellite image at 2200 UTC. Cloud formations viewed from Independence airport looking NW at 2240 UTC (middle) and looking SW at 2241 UTC 5 April 2006 (bottom). (Photos by Barrett Smith)

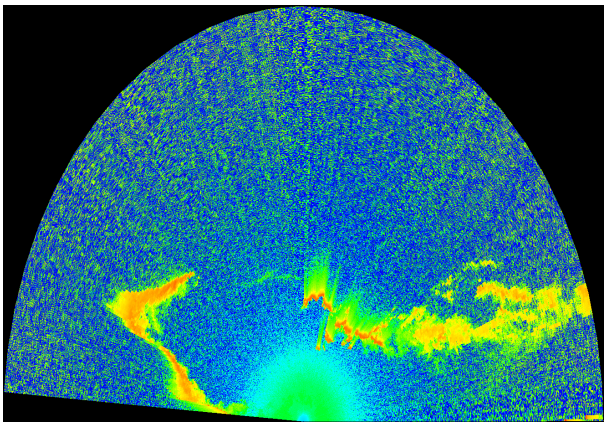

FIG. 9: Total reflectivity RHI scan from NCAR REAL at 22:41:52 UTC 5 April 2006.

Doyle (2008) of a gravity current which was responsible for westerly winds during SRP IOP 12. In that event, a cold front was located directly upstream of Owens Valley, which was key in explaining the mechanism for the gravity currents intrusion into the valley. In this case, the cold front was located well to the east, so an upstream cold air reservoir was not present and the onset mechanism is not clear.

While the westerly flow is initially confined to a gap jet originating from Kearsarge Pass, eventually west winds sweep across the entire valley as recorded by the observations. In particular, the specific pattern with higher winds in the northwest and southeast portions of the network are captured by the model (not shown). As the winds reach their maximum values, vertical cross-sections reveal a structure that is superficially similar to that seen in SRP IOP 16 (Fig. 10b) with a shallow layer of surface westerlies and turbulence and weaker winds above that. However, in this case, the higher TKE values are oriented along the top of the gravity current as opposed to vertically along the leading updraft. Furthermore, examining the onset of the flow in the 5 April event shows that the stagnant error in the middle of the valley has been lifted from the surface as opposed to forming during the flow evolution as in SRP IOP 16. While in many respects, the T-REX 5 April event is weaker than SRP IOP 16, the strong wind gusts and high TKE values still make it a significant westerly windstorm.

4. SUMMARY

SRP IOP 16 occurred as a cutoff low moved southward over the western US bring a cold air mass toward Owens Valley from the northeast. While trapped lee waves were present early in the event, surface heating allowed moderate westerlies to move into the valley before the flow evolved into a low-level wave breaking regime. During this time, strong surface gusts were observed, and deep updrafts and high TKE values were simulations. When the cold front passed through the field area, winds

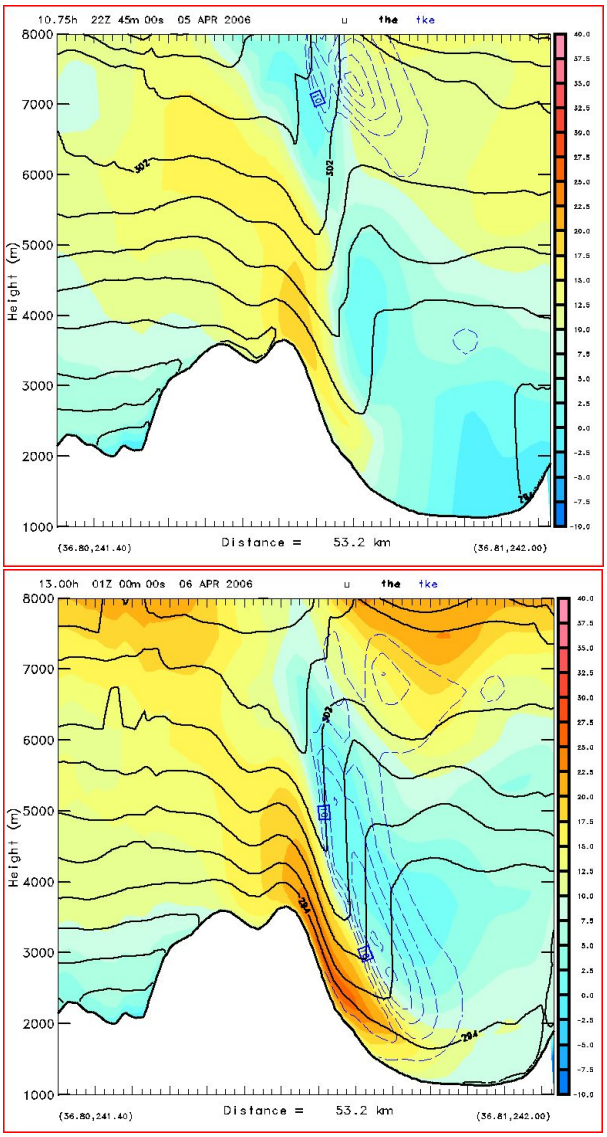

FIG. 10: Same as Fig. 7 for (top) 2200 UTC 5 April, (middle) 2245 UTC 5 April, and (bottom) 0100 UTC 6 April 2006.

shifted to northerlies which were nearly as strong as the winds earlier in the events.

During T-REX, on 5 April 2006, a westerly wind event occurred during the passage of a secondary trough associated with a storm system that had passed through the area on the previous two days. Visual evidence of both wave dynamics and convection were present in the valley, and the onset of the surface westerlies appeared to have the structure of an intruding density current. Again, strong surface winds were observed and high TKE values were simulated along the upper boundary of the surface westerlies, although the updrafts were not as deep in this case.

In many aspects, these cases are atypical of the mountain wave and rotor events observed in Owens Valley. However, they are still worthy of attention as part of a select number of cases featuring high winds of operational interest during this well-instrumented field campaign. Future work will continue to examine the events in this sample and attempt to determine the physical controls on their occurrence and intensity.

ACKNOWLEDGMENTS

The authors would like to thank all of the participants in the Sierra Rotors Project and Terrain-induced Rotor Experiment who helped to make these programs a success. For this study, we especially acknowledge Dr. Bill Brown of NCAR for providing the wind profiler plotting software and Barrett Smith of NWS Raleigh for help in clarifying the timing for the T-REX 5 April event. The primary sponsor of SRP and T-REX is the National Science Foundation. We would also like to acknowledge funding by the Office of Naval Research. COAMPS is a registered trademark of the Naval Research Laboratory.

REFERENCES

Grubišić, V., and B. J. Billings, 2007: The intense lee-wave rotor event of Sierra Rotors IOP 8. *J. Atmos. Sci.,* **64,** 4178-4201.

——-, and ——-, 2008: Summary of the Sierra Rotors Project wave and rotor events. *Atmospheric Science Letters,* **9,** 176-181.

——-, J. D. Doyle, J. Kuettner, R. Dirks, S. A. Cohn, L. L. Pan, S. Mobbs, R. B. Smith, C. D. Whiteman, S. Czyzyk, S. Vosper, M. Weissmann, S. Haimov, S. F. J. De Wekker, and F. K. Chow, 2008: The Terrain-induced Rotor Experiment. *Bull. Amer. Meteor. Soc.,* **89,** 1513-1533.

Hodur, R. M., 1997: The Naval Research Laboratory's Coupled Ocean/Atmosphere Mesoscale Prediction System (COAMPS). *Mon. Wea. Rev.,* **125,** 1414-1430.

Holmboe, J. R., and H. Klieforth, 1957: Investigation of mountain lee waves and the airflow over the Sierra Nevada. Final Report, Department of Meteorology, UCLA, Contract AF 19(604)-728, 283 pp.

Jiang, Q., and J. D. Doyle, 2008: Diurnal variation of downslope winds in Owens Valley during the Sierra Rotors experiment. *Mon. Wea. Rev.,* **136,** 3760-3780.

——-, ——-, S. Wang, and R. B. Smith, 2007: On boundary layer separation in the lee of mesoscale topography. *J. Atmos. Sci.,* **64,** 401-420.

Smith, R. B., 1985: On severe downslope winds. *J. Atmos. Sci.,* **42,** 2597-2603.